Brain imaging and lithium in bipolar disorder

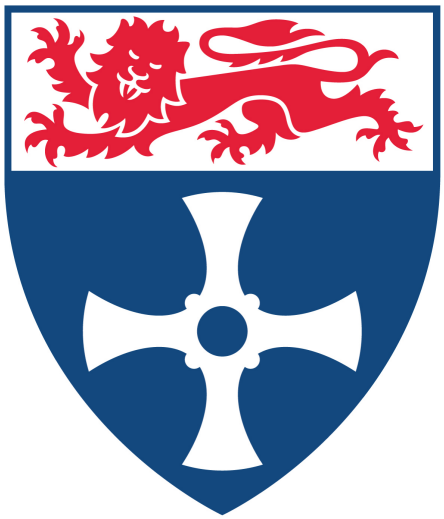

Joseph Hyman Necus

Translational and Clinical Research Institute
Newcastle University

This dissertation is submitted for the degree of
Doctor of Philosophy

November 2019

Abstract

Bipolar disorder is a major mental illness affecting 1% of the world's population and whilst numerous treatments are available, lithium retains a key position in major treatment guidelines. Despite its widespread clinical use, the mechanism of action of lithium is unknown. This thesis uses magnetic resonance imaging techniques in order to expand our understanding of where and how lithium acts within the brain with regards to structural abnormalities that occur in bipolar disorder.

The development of a novel imaging technique, ^{7}Li-MRI, has enabled researchers to non-invasively measure lithium distribution in the brain. However, the stability of lithium distribution over time is unknown. We investigated the scan-rescan comparability of this technique and showed that whilst ^{7}Li-MRI images exhibit high variability in terms of signal magnitude, the pattern of brain lithium distribution remains constant over one week.

To investigate previous findings which suggest an association between lithium use and increased white matter integrity we applied ^{7}Li-MRI alongside diffusion MRI to explore the spatial association between lithium distribution and white matter integrity in patients receiving treatment with lithium. Our findings revealed a positive association between local lithium signal and white matter integrity, adding support to findings which suggest that lithium exhibits a neuroprotective effect in white matter.

Using a quantitative imaging technique we identified elevated longitudinal relaxation in the brains of patients with bipolar disorder relative to controls. The biological underpinnings and potential for this technique to serve as a diagnostic biomarker are discussed.

In summary, using a range of magnetic resonance imaging acquisition techniques we have identified a number of structural brain differences between healthy subjects, lithium-treated patients and lithium-naïve patients.

Dedicated to my friends and family.

Acknowledgements

I am grateful for the funding and support received from the Reece Foundation and Medical Research Council who made this research possible. The Reece Foundation studentship has enabled me to devote my time to carrying out the research presented in this thesis and in particular facilitated the development of the Lithium Imaging in Controls (LiMRIC) study. Funding awarded to Dr David Cousins from the Medical Research Council enabled the development of the Bipolar Lithium Imaging and Spectroscopy Study, from which most of the data presented in this thesis was derived.

I would like to thank my co-authors Nishant Sinha, Carly Flowers, Fiona Smith, Peter Taylor, Peter Thelwall and Andrew Blamire for their insightful comments and suggestions during the preparation of manuscripts for submission. I am also particularly thankful to Amy-Rose Hayes for her help during the setup and screening of the LiMRIC study, a process which brought with it numerous challenges that were new to the both of us, and Attia Ahmad for her help with volunteer screening and bloodletting.

Finally, I would like to express my sincere gratitude to my primary supervisors Dr David Cousins and Dr Yujiang Wang. Throughout my PhD they have always been approachable and made time for me, and together make a motivational and supportive supervisory team.

Declaration

I hereby declare that except where speci c reference is made to the work of others, the contents of this dissertation are original and have not been submitted in whole or in part for consideration for any other degree or quali cation in this, or any other university. This dissertation is my own work and contains nothing which is the outcome of work done in collaboration with others, except as speci ed in the text and Acknowledgements.

Joseph Hyman Necus

November 2019

Publications

The following publications have been produced as part of work undertaken during the writing of this thesis:

Wang, Y.,Necus, J, Kaiser, M., Mota, B. (2016). Universality in human cortical folding in health and disease. Proceedings of the National Academy of Sciences of the United States of America, 113(45), 12820-12825.

Smith, F. E., Thelwall, P. E,Necus, J.,Flowers, C. J., Blamire, A. M., Cousins, D. A. (2018). 3D ^{7}Li magnetic resonance imaging of brain lithium distribution in bipolar disorder. Molecular Psychiatry, 23(11), 2184-2191.

Necus, J.,Sinha, N., Smith, F. E., Thelwall, P. E., Flowers, C. J., Taylor, P. N., Blamire, A. M., Cousins, D. A., and Wang, Y. (2019). White matter microstructural properties in bipolar disorder in relationship to the spatial distribution of lithium in the brain. Journal of Affective Disorders, 253:224–231.

Wang, Y.,Necus, J.,Rodriguez, L. P., Taylor, P. N., Mota, B., Universality in human cortical folding across lobes of individual brains. (2019). Communications Biology. 2:191.

Necus, J.,Smith, F. E., Thelwall, P. E., Flowers, C. J., Sinha, N. , Taylor, P. N., Blamire, A. M., Wang, Y. and Cousins, D. A. (2019), Quanti cation of brain proton longitudinal relaxation (T1) in lithium-treated and lithium-naïve patients with bipolar disorder in comparison to healthy controls. Bipolar Disord. Accepted Author Manuscript. doi:10.1111/bdi.12878

Table of contents

List of gures xvii

List of tables xix

Nomenclature xxi

1 Introduction 1
1.1 Bipolar Disorder 1
1.1.1 Diagnosis 2
1.1.2 Structural abnormalities in Bipolar Disorder 6
1.2 Lithium therapy in Bipolar Disorder 9
1.2.1 Discovery and use of lithium 9
1.2.2 Mechanism of action 11
1.3 Lithium distribution 14
1.3.1 Histological studies 15
1.3.2 ^{7}Lithium Magnetic Resonance Spectroscopy 16
1.3.3 ^{7}Lithium Magnetic Resonance Imaging 18
1.4 Summary and aims of this thesis 20

2 Magnetic Resonance Image analysis 21
2.1 Overview 21
2.2 T_1 and T_2 weighted images 21
2.2.1 Uses of T_1w and T_2w images 22
2.2.2 Limitations 25
2.3 Quantitative relaxometry 25
2.3.1 Uses of qMRI 28

2.3.2 Limitations . . . 28
2.4 Diffusion MRI . . . 29
2.4.1 Uses of dMRI . . . 30
2.4.2 Limitations . . . 33
2.5 ^{7}Li-MRI . . . 33
2.6 Discussion . . . 35

3 LiMRIC 37
3.1 Abstract . . . 37
3.2 Background . . . 38
3.3 Methods . . . 39
3.3.1 Participants . . . 39
3.3.2 Image acquisition . . . 40
3.3.3 Image processing and analysis . . . 42
3.4 Results . . . 44
3.4.1 ^{7}Li-MRI raw scans . . . 44
3.4.2 Serum lithium concentration . . . 49
3.4.3 Variability in ^{7}Li-MRI signal intensity . . . 49
3.4.4 Scan-rescan reliability . . . 51
3.5 Discussion . . . 57
3.5.1 ^{7}Li-MRI raw intensity . . . 57
3.5.2 ^{7}Li-MRI scan-rescan reliability . . . 57
3.5.3 Lithium distribution within versus between subject comparison . . . 59
3.5.4 Conclusions . . . 60

4 ^{7}Li-MRI and Generalised Fractional Anisotropy 61
4.1 Abstract . . . 62
4.2 Background . . . 62
4.3 Methods . . . 64
4.3.1 Subjects and assessments . . . 64
4.3.2 Group comparison . . . 66
4.3.3 Image acquisition . . . 66
4.3.4 Image processing and analysis . . . 67
4.3.5 T_1w image processing . . . 67

4.3.6 Diffusion-weighted image processing 68
4.3.7 ^{7}Li-MRI image processing 69
4.3.8 Supplementary FA analysis 70
4.4 Results 72
4.4.1 Group characteristics 72
4.4.2 Mean white matter gFA comparison between groups 75
4.4.3 Region of interest gFA group comparison 75
4.4.4 Co-localisation of lithium and gFA 79
4.5 Discussion 82

5 Brain T_1 in Bipolar Disorder 87
5.1 Abstract 87
5.2 Background 88
5.3 Methods 89
5.3.1 Participants 89
5.3.2 MRI acquisition 90
5.3.3 Image processing and analysis 91
5.4 Results 93
5.4.1 Group characteristics 93
5.4.2 Group comparison of T_1 times across tissue types 95
5.4.3 Investigation of regional effects 96
5.5 Discussion 99

6 Discussion 103
6.1 Summary of key findings and implications 103
6.2 Challenges faced during this thesis 104
6.3 Future challenges 106
6.4 Concluding remarks 109

Appendix A The relationship between ^{7}Lithium and Fractional Anisotropy 111
A.1 Summary of FA analysis results 111
A.2 Mean white matter FA comparison between groups 112
A.3 Region of interest FA group comparison 112
A.4 Co-localisation of lithium and FA 115

A.5 Linear mixed effect modelling of the relationship between FA and ^{7}Li-MRI signal 118
A.6 Linear mixed effect analysis for other ^{7}Li-MRI voxel WM percentages . . . 119

Appendix B T_1 in Desikan-Killiany, Destrieux and JHU atlases 121
B.1 Desikan-Killiany atlas 121
B.1.1 Raw Desikan-Killiany ROI effect sizes and p-values 121
B.1.2 Effect of ROI erosion on Desikan-Killiany ROI effect sizes 124
B.2 Destrieux atlas 126
B.3 JHU atlas 130

References 135

List of gures

1.1 ^{7}Li-MRI 19

2.1 T_1w and T_2w images 23
2.2 Freesurfer cortical surface reconstruction and subcortical segmentation . . . 25
2.3 Inversion recovery method to measure T_1 26
2.4 Example dMRI study work ow 33
2.5 ^{7}Li-MRI resolution and partial volume effects 34

3.1 LiMRIC experimental design 40
3.2 LiMRIC scan protocol 42
3.3 LiMRIC within vs. between subject schematic 44
3.4 Subject MR02 raw ^{7}Li-MRI scans 45
3.5 Subject MR03 raw ^{7}Li-MRI scans 46
3.6 Subject MR04 raw ^{7}Li-MRI scans 47
3.7 Subject MR05 raw ^{7}Li-MRI scans 48
3.8 LiMRIC ^{7}Li-MRI signal intensity 50
3.9 LiMRIC effect of repositioning in scanner 52
3.10 LiMRIC correlation of co-registered ^{7}Li-MRI brain voxels between days 7, 8 and 14 54
3.11 LiMRIC within vs between subject correlations 56

4.1 ^{7}Li-MRI and gFA processing pipeline 71
4.2 gFA mean group comparison 75
4.3 gFA ROI effect sizes 76
4.4 Relationship between ^{7}Li signal amplitude and gFA 80

5.1 Detrended T_1 values by group and tissue class 96

5.2 Distribution of effect sizes (BDL < BDC) for all Desikan-Killiany regions of interest (ROI), segregated by tissue type 97
5.3 Distribution of effect sizes (BD > HC) for all Desikan-Killiany regions of interest (ROI), segregated by tissue type 97
5.4 Effect sizes (Cohen's d) and signi cance testing for BD > HC comparison in Desikan-Killiany regions of interest (ROI) 98

A.1 FA mean group comparison 112
A.2 Region-wise FA effect sizes (BDL > BDC) 113
A.3 Relationship between lithium signal amplitude and FA 117

B.1 Example of ROI erosion on cortical ROIs 125
B.2 Effect of ROI erosion on effect sizes 125
B.3 BD > HC T_1 comparison using Destrieux parcellation 126
B.4 BD > HC T_1 comparison using JHU white matter atlas 130

List of tables

3.1 LiMRIC serum lithium concentrations 49

4.1 ^{7}Li-MRI / gFA subject characteristics 73
4.2 ^{7}Li-MRI / gFA subject medication use 74
4.3 BDL > BDC gFA effect sizes for JHU ROIs 78
4.4 gFA slope estimates per %WM 81
4.5 Theoretical Likelihood Ratio Test (75-100% WM, random slope vs random intercept models) 81

5.1 Subject characteristics 94
5.2 Medication use by class 95
5.3 Detrended T_1 by subject group per tissue type 95

A.1 BDL > BDC FA effect sizes for JHU ROIs 115
A.2 Theoretical Likelihood Ratio Test (75-100% WM, random slope models) . 118
A.3 Theoretical Likelihood Ratio Test (75-100% WM, random slope vs random intercept models) 118
A.4 FA slope estimates per %WM 119

B.1 Effect size (Cohen's d), and signi cance testing for BD>HC comparison for each region of interest (excluding cerebellum) in the Desikan-Killiany atlas 124
B.2 Effect size (Cohen's d), and signi cance testing for BD>HC comparison for each region of interest (excluding cerebellum) in the Destrieux atlas. 129
B.3 JHU atlas T_1 effect size table 134

Nomenclature

Greek Symbols

c^2 Chi Squared

r Rho

Acronyms / Abbreviations

AMI Affective Morbidity Index

bSSFP Balanced Steady State Free Precession

ConLiGen The International Consortium for Lithium Genetics

CSF Cerebrospinal uid

DESPOT1 Driven Equilibrium Single Pulse Observation of T_1

DMI Depression-Mania-Free Interval

dMRI Diffusion MRI

DSM-5 Diagnostic and Statistical Manual of Mental Disorders Version 5

ENIGMA Enhancing Neuro Imaging Genetics through Meta Analysis

FA Fractional Anisotropy

FLAIR Fluid Attenuated Inversion Recovery

FLIRT FMRIB's Linear Image Registration Tool

FMRIB Oxford Centre for Functional MRI of the Brain

FNIRT FMRIB's Non Linear Image Registration Tool

FSL FMRIB's software library

gFA Generalised Fractional Anisotropy

GM Grey Matter

GSK-3β Glycogen Synthase Kinase 3β

JHU John Hopkins University

LiMRIC Lithium Imaging in Controls

MDI Mania-Depression-Free Interval

MNI Montreal Neurological Institute

MRI Magnetic Resonance Imaging

MRS Magnetic Resonance Spectroscopy

NMR Nuclear Magnetic Resonance

ROI Region of interest

SPGR Spoiled Gradient Recalled Echo

T_1w T_1 weighted

T_2w T_2 weighted

TR Repetition Time

WM White Matter

YMRS Young Mania Rating Scale

Chapter 1

Introduction

1.1 Bipolar Disorder

Bipolar disorder is a mental illness with an unknown aetiology. It has a prevalence of approximately 1% in the population and is a leading cause of disability worldwide (Krahn, 2011). Owing to the early onset (median age of 25 years), severity, and chronic nature of bipolar disorder, it is reported to be responsible for the loss of more disability-adjusted life years than diseases such as Alzheimer's disease, epilepsy and all forms of cancer (Merikangas et al., 2011).

Bipolar disorder is characterised by the experience of depressive and manic episodes, and sufferers are more likely to commit suicide. Treatment with lithium is an effective way of managing episodes and preventing relapse in patients with bipolar disorder, additionally reducing suicidal behaviour. However, it is not known how lithium works, nor why it is an effective treatment in some individuals but not others. A greater understanding of how lithium exerts its therapeutic effects might provide insights into the pathophysiology of bipolar disorder, or separate out a subgroup of lithium responders with different illness characteristics and underlying pathology.

1.1.1 Diagnosis

Diagnosis of bipolar disorder is distinguished from other affective disorders such as major depressive disorder by patients experiencing manic and/or hypomanic episodes. The term bipolar disorder is used to describe a range of related disorders consisting of multiple sub-types. The two main sub-types of bipolar disorder listed in the Diagnostic and Statistic Manual Version 5 (DSM-5) are Bipolar Disorder Type I and Bipolar Disorder Type II (American Psychiatric Association, 2013):

- Bipolar Disorder Type I is characterised by the experience of mania. The manic episode may have been preceded by and may be followed by hypomanic or major depressive episodes. The lifetime prevalence of BD Type I is estimated to be 0.6%.
- Bipolar Disorder Type II is characterised by the experience of hypomania and depression; the experience of a manic episode would rule out Type II diagnosis and elevate the diagnosis to Type I. The lifetime prevalence of BD Type II is estimated to be 0.4%.

Individuals with bipolar disorder are at an increased risk of suicide and experience cognitive impairment; although this is not currently part of the diagnostic criteria. The DSM-5 criteria for manic, hypomanic and depressive episodes are given in Boxes 1-3 on pages 3, 4 and 5, respectively. Whilst the DSM-5 specifies other subtypes of bipolar disorder such as cyclothymic disorder, medication-induced bipolar disorder and “other specified and related disorder”, the data presented and discussed in this thesis is primarily concerned with Type I and Type II manifestations of bipolar disorder.

Bipolar disorder is a highly recurrent disorder. It has been reported that the average duration of episodes last between two to seven months (Angst and Sellaro, 2000), though this can vary significantly between individuals, and recurrences tend to become closer together as the disorder progresses (Haldipur, 1999). Successful response to treatment is therefore reflected by an increase in the duration of time between episodes. Whilst bipolar disorder was considered historically as a “functional psychosis” primarily caused by neurochemical derangement, it is now becoming clear that there are underlying structural changes and perhaps even progressive changes in brain structure and function that occur during the course of bipolar disorder (Schneider et al., 2012).

Box 1. Criteria for a manic episode.

(A) Distinct period of abnormally and persistently elevated, expansive, or irritable mood and abnormally and persistently increased activity or energy, lasting at least 1 week and present most of the day, nearly every day (or any duration if hospitalisation is necessary).

(B) During the period of mood disturbance and increased energy and activity, three (or more) of the following symptoms (four if the mood is only irritable) are present to a signi cant degree and represent a noticeable change from usual behaviour:

- In ated self-esteem or grandiosity
- Decreased need for sleep (e.g. feels rested after only 3 hours of sleep)
- More talkative than usual or pressure to keep talking
- Flight of ideas or subjective experience that thoughts are racing
- Distractibility (i.e, attention too easily drawn to unimportant or irrelevant external stimuli), as reported or observed
- Increase in goal-directed activity (either socially, at work or school, or sexually) or psychomotor agitation
- Excessive involvement in activities that have a high potential for painful consequences (e.g. engaging in unrestrained buying sprees, sexual indiscretions, or foolish business investments)

(C) The mood disturbance is suf ciently severe to cause marked impairment in social or occupational functioning or to necessitate hospitalisation to prevent harm to self or others, or there are psychotic features.

(D) The episode is not attributable to the physiological effects of a substance (eg, a drug of abuse, a medication, other treatment) or to another medical condition.

Box 2. Criteria for a hypomanic episode.

(A) A distinct period of abnormally and persistently elevated, expansive, or irritable mood and abnormally and persistently increased activity or energy, lasting at least 4 consecutive days and present most of the day, nearly every day.

(B) During the period of mood disturbance and increased energy and activity, three (or more) of the following symptoms (four if the mood is only irritable) have persisted, represent a noticeable change from usual behaviour, and have been present to a signi cant degree:

- In ated self-esteem or grandiosity
- Decreased need for sleep (e.g. feels rested after only 3 hours of sleep)
- More talkative than usual or pressure to keep talking
- Flight of ideas or subjective experience that thoughts are racing
- Distractibility (i.e. attention too easily drawn to unimportant or irrelevant external stimuli), as reported or observed
- Increase in goal-directed activity (either socially, at work or school, or sexually) or psychomotor agitation
- Excessive involvement in activities that have a high potential for painful consequences (e.g. engaging in unrestrained buying sprees, sexual indiscretions, or foolish business investments)

(C) The episode is associated with an unequivocal change in functioning that is uncharacteristic of the individual when not symptomatic.

(D) The disturbance in mood and the change in functioning are observable by others.

(E) The episode is not severe enough to cause marked impairment in social or occupational functioning or to necessitate hospitalisation. If there are psychotic features, the episode is, by de nition, manic.

(F) The episode is not attributable to the physiological effects of a substance (e.g. a drug of abuse, a medication, other treatment).

Box 3. Criteria for a major depressive episode.

(A) Five (or more) of the following symptoms have been present during the same 2-week period and represent a change from previous functioning; at least one of the symptoms is either (1) depressed mood or (2) loss of interest or pleasure:

- Depressed mood most of the day, nearly every day, as indicated by either subjective report (e.g., feels sad, empty, or hopeless) or observation made by others (e.g. appears tearful). (Note: In children and adolescents, can be irritable mood.)
- Markedly diminished interest or pleasure in all, or almost all, activities most of the day, nearly every day (as indicated by either subjective account or observation).
- Signi cant weight loss when not dieting or weight gain (e.g. a change of more than 5% of body weight in a month), or decrease or increase in appetite nearly every day. (Note: In children, consider failure to make expected weight gain.)
- Insomnia or hypersomnia nearly every day.
- Psychomotor agitation or retardation nearly every day (observable by others; not merely subjective feelings of restlessness or being slowed down).
- Fatigue or loss of energy nearly every
- Feelings of worthlessness or excessive or inappropriate guilt (which may be delusional) nearly every day (not merely self-reproach or guilt about being sick).
- Diminished ability to think or concentrate, or indecisiveness, nearly every day (either by subjective account or as observed by others).
- Recurrent thoughts of death (not just fear of dying), recurrent suicidal ideation without a speci c plan, or a suicide attempt or a speci c plan for committing suicide.

(B) The symptoms cause clinically signi cant distress or impairment in social, occupational, or other important areas of functioning.

(C) The episode is not attributable to the physiological effects of a substance or another medical condition.

The aetiology of bipolar disorder remains incompletely de nes and clinical heterogeneity presents a challenge with regards to understanding this. There may be a common cause with differing manifestations or several pathologically distinct conditions with overlapping presentations. Whilst it is dif cult to disentangle cause from consequence when it comes to biological differences between patients and healthy individuals, it is evident that patients with bipolar disorder exhibit a number of structural brain abnormalities.

1.1.2 Structural abnormalities in Bipolar Disorder

A considerable amount of research has been undertaken in order to try and identify structural and functional changes in the brains of patients with bipolar disorder. In doing so it is hoped that such differences will provide insights into the pathophysiology of bipolar disorder, enable earlier diagnosis, targeted intervention, and provide a basis for the development of new treatments. One of the main tools of assessing structural and functional brain changes in vivo is via Magnetic Resonance Imaging (MRI). The following section aims to introduce what neuroimaging techniques have revealed about some of the most commonly identi ed structural changes that occur in the brain during bipolar disorder. More detailed information regarding the neuroimaging methods themselves can be found in Chapter 2.

Ventricles

Ventriculomegaly, a term used to describe enlargement of the ventricles, is a feature which has been repeatedly found to be present in patients with bipolar disorder. Results from a meta-analysis of studies which have used MRI to assess brain morphometry in bipolar disorder suggest that patients consistently exhibit an increased ventricle to brain ratio in the right lateral ventricle, with other ventricles exhibiting greater heterogeneity in terms of enlargement (McDonald et al., 2004). Moreover, there is also evidence to suggest that the lateral ventricles are larger in patients who have experienced multiple episodes relative to rst-episode patients (Strakowski et al., 2002) and in patients with BD Type I vs Type II (Hibar et al., 2016). However, whilst ventricular enlargement is a feature which is relatively easy to detect using structural MRI, it is not a feature speci c to bipolar disorder. Ventriculomegaly is common to a range of neurological disorders and is perhaps most apparent and more commonly associated with dementia (Forstl et al., 1995). As a result, this makes it dif cult to attribute a speci c link between ventriculomegaly and bipolar disorder.

Grey matter

There is substantial evidence from a large number of independent studies to suggest that patients with bipolar disorder exhibit a widespread reduction in grey matter volume (Abé et al., 2016; Bora et al., 2010; Foland-Ross et al., 2011; Hibar et al., 2017, 2016). In a meta analysis published by the ENIGMA consortium which included the analysis of 1837 MRI images from patients with bipolar disorder and 2582 unrelated adult healthy controls, it was concluded that in terms of changes in cortical thickness, patients exhibit the greatest magnitude of cortical thinning in the left pars opercularis, left fusiform gyrus and left rostral middle frontal cortex (Hibar et al., 2017). In terms of subcortical grey matter volume, the same group report sign cant reductions in volume bilaterally in the amygdala, hippocampus and thalamus (Hibar et al., 2016). However, as with vectricular enlargement, widespread reductions in grey matter volume is another feature that is common to a number of neurological conditions and therefore non-speci c to bipolar disorder. Moreover, it is possible that these two ndings are inter-related, as loss of subcortical volume surrounding the ventricles will present itself as ventricular enlargement. Attempts to classify patients from controls based upon such morphometric data have thus far been unsuccessful, yielding low classi cation accuracy (65%), thereby highlighting the lack of speci city of this structural feature with regards to bipolar disorder (Nunes et al., 2018).

White matter

Whilst changes in grey matter volume have received considerable attention throughout the bipolar disorder literature, until relatively recently less work had been performed to investigate changes in white matter structure. Perhaps the rst recognition of white matter abnormalities in bipolar disorder can be attributed to the identi cation of an increased frequency of white matter hyperintensities (WMH), which appear as bright spots within white matter (Figiel et al., 1991). An increased frequency of WMH in bipolar disorder is a feature which has been replicated numerous times throughout the literature, with this effect being seen across all age ranges (Aylward et al., 1994; Dupont et al., 1995; Lloyd et al., 2009; Regenold, 2008; Videbech, 1997). However, WMHs are also found to be more common in older individuals during healthy ageing and a link between WMHs and the pathophysiology of BD has yet to be established.

The development of a technique known as diffusion MRI (for further details see section 2.4) enables the examination of the microstructural properties of tissue by mapping water molecule diffusion. In pure fluid states, water diffuses equally in all directions (isotropic), whilst in neurons water cannot readily cross the hydrophobic myelin sheaths and diffusion is restricted (anisotropic) along the direction of the axon. The parallel configuration of axons in white matter renders this directional diffusion detectable at the microstructural scale, reflected in the dMRI-derived parameter of fractional anisotropy (FA). Reductions in FA have been shown to correspond with demyelination and axonal injury (Boretius et al., 2012; Song et al., 2002). Patients with bipolar disorder have been shown to exhibit decreased FA within white matter (Adler et al., 2006; Benedetti et al., 2011; Bruno et al., 2008; Favre et al., 2019) and a meta analysis of whole brain voxel-wide FA studies has identified two significant clusters near the right parahippocampal gyrus and right subgenual cingulate cortex which exhibit consistently reduced FA during bipolar disorder (Vederine et al., 2011). In addition to regional white matter damage, alterations in whole brain connectivity have been identified during bipolar disorder (Collin et al., 2016). This study found a reduction in the connectivity strength of inter-hemispheric connections in patients diagnosed with bipolar disorder type I relative to healthy controls.

T_1 relaxation

Longitudinal relaxation (T_1) is a biophysical property of protons which is sensitive to tissue properties including myelin, macromolecular content, iron and water. “Quantitative relaxometry” describes a field of study in which imaging techniques may be used to quantify this T_1 property (for further details regarding this technique see section 2.3). There is some evidence from studies employing relaxometry to suggest that patients with bipolar disorder exhibit differences in proton relaxation times within the brain. For example, longitudinal relaxation (T_1) within the frontal and temporal lobes has been shown to be higher in patients with bipolar disorder (Rangel-Guerra et al., 1983). Elevated T_1 is associated with lower myelin content, supporting the finding that reductions in white matter integrity occur during bipolar disorder. Whilst this report of elevated T_1 in bipolar disorder is an old observation, the development of high resolution quantitative mapping techniques are beginning to attract more attention, leading to the identification of novel findings and development of new hypotheses. For example, recent studies employing a quantitative T_1 mapping technique (a parameter

sensitive to T_1) have found that T_1r is higher in cerebral and cerebellar white matter in patients with bipolar disorder compared to controls (Johnson et al., 2018, 2015).

Summary

A large number of structural brain changes have been identi ed in bipolar disorder, however, changes which are speci c to bipolar disorder have yet to be found. As a result, it is currently not possible to diagnose and treat patients based solely upon observable structural brain changes. Despite this, structural changes have already provided a number of insights into the potential pathophysiology of bipolar disorder. Moreover, by characterising such differences, researchers can begin to investigate whether novel or existing therapies are able to prevent or reverse such changes. In doing so, this may reveal more about the mechanism of action of such treatments, whilst also holding the potential to further understand why certain treatments work in certain subsets of patients.

1.2 Lithium therapy in Bipolar Disorder

Whilst there are now a range of treatments available during the management of bipolar disorder, lithium, which is cited as the rst drug to be used in all of modern psychiatry, remains the rst line treatment for bipolar disorder (Shorter, 2009). Lithium has been shown to be effective at treating both manic (Poolsup and de Oliveira, 2000) and depressive episodes (Nolen and Bloemkolk, 2000), and effectively reduces the risk of suicide (Cipriani et al., 2005). The following section introduces the discovery and clinical use of lithium during bipolar disorder, and provides an overview of research into lithium's mechanism of action.

1.2.1 Discovery and use of lithium

Discovery of lithium

The rst medicinal use of lithium was recognised as far back as the mid 19th century. During this time Alexander Ure recognised the ability of lithium to bind to uric acid and in turn advocated the use of lithium as a treatment for bladder stones caused by the crystallisation of uric acid. At around the same time the English physician Alfred Garrod noted high

levels of uric acid in his patients with gout (Garrod, 1860) and subsequently popularised the treatment of gout and “brain gout” using lithium, thereby marking itself as an early reference to potential use of lithium for psychiatric purpose.

Throughout the latter half of the 19th century a number of references to the use of lithium for psychiatric purposes may be found. For example, references were made to the use of lithium bromide as an anticonvulsant (Mitchell, 1870), and later on for its ef cacy in treating “general nervousness” (Mitchell, 1877). However, it wasn't until the end of the 19th century before the use of lithium became recognised for its ef cacy at treating depressive symptoms; this came when the Danish psychiatrist Frederik Lange reported on the use of lithium during the treatment of “melancholic depression” (Schioldann, 2001).

The recognition of the use of lithium during the treatment of mania did not come about until the middle of the 20th century. This occurred when the Australian psychiatrist John Cade (Cade, 1949) hypothesised that some of his patients' “psychotic excitement” could be attributed to abnormally high uric acid levels. Cade noted that following the treatment of his patients with combinations of lithium citrate and lithium carbonate, a subset of patients responded extremely well to treatment, exhibiting a dramatic reduction in their manic symptoms.

Despite the discovery made by Cade in 1949, lithium was not of cially approved by the American Food and Drug Administration until 1970. This failure to approve lithium is thought to be in part due to a concurrent report on lithium's toxicity during its use as a table salt substitute for patients with congestive heart failure (Corcoran and Page, 1949). In the period leading up to 1970 lithium was prescribed without FDA approval by a number of American physicians (Shorter, 2009); however, the fact that lithium was not of cially approved by the FDA meant that the ef cacy and safety of lithium could not be established by scientists working in the US. Despite its ban in the US, experiments with lithium continued to be trialled by a small number of psychiatrists in Europe (Schou and Mogens, 1958). The ef cacy of lithium treatment as a means of treating acute mania was easy to replicate, however, proof of it's ef cacy during relapse prevention took much longer to become widely accepted. Owing to the continuous replication of positive ndings regarding the bene ts of lithium use during the treatment of mania and relapse prevention, lithium therapy remains the gold standard treatment for bipolar disorder today.

Clinical use

Lithium is administered orally as it is easily absorbed by the gut. During lithium therapy serum lithium concentration is aimed to be kept between the therapeutic range of 0.6 - 0.8 mmol/L (or 0.8 - 1.0 mmol/L in severe cases or non-responders) and patients must be closely monitored in order to avoid lithium toxicity (Goodwin et al., 2016). Serum lithium concentration can be measured with con dence and ease by testing blood samples (Alda and Martin, 1988). However, although the monitoring of serum levels is used to minimise the risk of toxicity, it does not guarantee therapeutic response. Moreover, in certain cases patients can exhibit signs of lithium toxicity when serum concentrations are within the target therapeutic range. Whilst the mechanism of toxicity occuring within the therapeutic range is unknown, techniques which enable quanti cation of brain lithium levels *in vivo* such as ^{7}Li-MRS (see section 1.3.2) have been used to attempt to determine the relationship between serum and brain lithium concentration with the aim of trying to understand whether this relationship is related to toxicity and therapeutic response.

1.2.2 Mechanism of action

Despite its widespread use, lithium's exact mechanism of action remains elusive. The actions of lithium at a cellular level are manyfold and several effects have been well characterised. The following section provides an overview of some of the biological actions of lithium alongside evidence relating to their potential ef cacy during the treatment of bipolar disorder.

Effect on neurotransmission

The effects of lithium on neurotransmitter systems have been investigated and characterised in both preclinical and clinical studies. The focus of this work has been on monoaminergic systems, owing to their importance in mood regulation. Lithium augments serotonergic neurotransmission (Blier and De Montigny, 1985) and this effect may be important in its antidepressant action and possibly in its ability to reduce suicidal behaviours. As lithium attenuates some of the psychoactive effects of amphetamines (Vankammen and Murphy, 1975), its effects on dopaminergic neurotransmission have received considerable attention. Evidence from microdialysis studies suggest that the anti-manic effects of lithium may be

due to a reduction in presynaptic dopamine release (Ferrie et al., 2005, 2006). The effects of lithium administration on noradrenergic neurotransmission appear more mixed, with some evidence to suggest that the effect of lithium on noradrenaline excretion may depend upon mood state (Beckmann et al., 1975; Bowers and Heninger, 1977; Greenspan et al., 1970). Together, such findings have led to the suggestion that lithium may work via the modulation of monoaminergic pathways (Baptista et al., 1993; Ferrie et al., 2008). However, the complex way in which lithium affects such systems, combined with the technical difficulty associated with quantifying neurotransmission *in vivo*, means that a comprehensive understanding of the way in which lithium modulates neurotransmission on a whole systems level is still lacking.

Effect on secondary messengers

Lithium has been shown able to modulate the concentration of cellular signalling molecules which are important for maintaining neuronal integrity and promoting synaptic plasticity. The detection of molecular compounds can be achieved *in vivo* using a technique known as Magnetic Resonance Spectroscopy (see section 1.3.2 for details) and this technique has been used to study how the concentration of a range of compounds differ during bipolar disorder. For example, lithium administration has been linked with an increased concentration of the compound N-acetylaspartate (NAA) (Moore et al., 2000a), a cellular marker of neuronal integrity. During this study associations between lithium use and increased NAA were identified in regions which exhibited greatest grey matter density. The relationship between lithium use and the concentration of the compound myo-inositol has gained particular interest throughout the lithium literature. An apparent ability of lithium to reduce the cellular content of myo-inositol has led this effect to become known as the “inositol depletion hypothesis” (Allison and Stewart, 1971). During preclinical experiments, lithium administration has been shown to increase the spread of axonal growth cones (Williams et al., 2002), an effect which was reversed following the addition of myo-inositol (Harwood, 2005; Shaltiel et al., 2007), suggesting that the relationship between lithium and myo-inositol may play a role during the facilitation of synaptic plasticity. However, debate still remains as to whether lithium does in fact augment myo-inositol (Moore et al., 1999), or rather decreases it (Forester et al., 2008); it is possible that acute administration of lithium decreases myo-inositol levels with the reverse effect occurring following chronic administration.

Neuroprotection

Lithium has repeatedly been reported to exhibit neuroprotective (Forlenza et al., 2014), neurotrophic (Quiroz et al., 2010) and neuroplastic (Gray and McEwen, 2013) properties. For example, during preclinical studies it has been shown that lithium inhibits the apoptotic enzyme Glycogen Synthase Kinase (GSK-3β). Whilst the precise mechanism of inhibition is unknown, this may occur via competition with Mg^{2+} as a co-factor (Freland and Beaulieu, 2012). GSK-3β is an enzyme expressed widely throughout body and brain tissue and is involved in the phosphorylation of compounds leading to their inactivation or degradation. Upregulation of GSK-3β activity is associated with neuronal apoptosis (Hetman et al., 2000), and hence inhibition of this enzyme by lithium can protect against cell death. As well as being able to inhibit the processes preceding apoptosis, lithium administration has also been shown to actively promote cell proliferation. However, it is yet unclear whether such proliferation translates into fully differentiated functional neurons downstream (Agam et al., 2015; Zanni et al., 2017).

There is evidence from imaging studies to suggest that this ability of lithium to down-regulate apoptosis and promote proliferation on a cellular level might lead to effects that are detectable on a macro-scale. Multiple studies have shown using MRI that there is an association between the use of lithium and an increased volume of grey matter (Bearden et al., 2008; Cousins et al., 2013; Hibar et al., 2017; Lyoo et al., 2010; Monkul et al., 2007; Moore et al., 2000b; Yucel and MacQueen, 2008; Zung et al., 2016). This widely replicated association between lithium and increased grey matter volume has led to the suggestion that lithium may protect against or even reverse grey matter changes that are known to occur during bipolar disorder (Hibar et al., 2016). However, it has also been suggested that the association between increased MRI measures of grey matter volume and lithium use may in fact be an imaging artefact stemming from the ability of lithium to shorten proton longitudinal relaxation (T_1). Lithium administration in healthy individuals has been shown to reduce T_1 times in grey matter (Cousins et al., 2013), a phenomenon which is also known to occur in vitro when lithium is added to aqueous solution (Fabricand and Goldberg, 1967). In a study showing elevated $T_1\rho$ values in patients relative to controls, when patients were subdivided according to medication use, it was found that patients using lithium exhibited lower $T_1\rho$ values than patients using other medications; however, this finding was not replicated in a later study (Johnson et al., 2018). In addition to a potential neuroprotective action in the cortex, there is growing evidence to suggest an association between lithium use and protection of white

matter structure. Patients with bipolar disorder undergoing lithium treatment have been shown to exhibit higher white matter integrity relative to those treated with other medications (Gildengers et al., 2015; Haarman et al., 2016; Macritchie et al., 2009; Sussmann et al., 2008), and lithium has been shown to protect against reductions in white matter volume (Berk et al., 2017). In Chapter 4 we investigate the association between lithium use and white matter structure.

1.3 Lithium distribution

The prevailing inability to establish a clear link between the actions of lithium at a cellular and systems level and its therapeutic properties suggests that lithium may not have a single, targeted action during bipolar disorder. Instead an understanding of the actions of lithium may be better framed in the same way as other common biologically active ions. After all, the pharmacokinetic properties of lithium resembles other monovalent cations, and unlike most pharmaceutical compounds lithium is not metabolised (Ward et al., 1994). Recognition of lithium as an ion warrants the need for a concrete characterisation of lithium's distribution throughout bodily tissues as it is clear that the distribution of ions is closely related to their functions. For example, 99% of all calcium occurs in the skeleton (Bessey et al., 1935), 90% of potassium is located intracellularly whereby it is important for maintaining resting state potential (Palmer and Clegg, 2016), and 90% of sodium is located within extracellular uid whereby it facilitates the generation of action potentials (Deane and Smith, 1952).

It is notable that while large quantities of such ions appear to concentrate in certain regions, the remaining percentages also perform essential functions. For example, although 99% of calcium occurs within bone, the remaining 1% is involved during a range of processes including muscle contraction, respiration and long term potentiation (Clapham, 1995). Thus, calcium exhibits non-uniform distribution and multi-functional properties. Lithium has a disproportionately large hydration shell which restricts its ionic mobility in biological systems, with some arguing that it has characteristics more closely comparable to calcium and magnesium rather than sodium and potassium (Stern and Amis, 1959). Consistent with this, lithium has been shown to accumulate in bone (Birch, 1976; Birch and Jenner, 1973), whereby its accumulation is accompanied by a decrease in calcium concentration, and there is evidence to suggest that a fraction of lithium incorporated into bone remains for at least

nine months following discontinuation (Birch and Hullin, 1972). Based on the assumption that lithium behaves similarly to other biologically active cations it may be hypothesised that lithium is multi-functional, exhibits an uneven distribution throughout the body, and that the distribution of lithium is related to it's function.

Although it is generally accepted that the actions of lithium which underpin its ef cacy during bipolar disorder occur within the brain, little work has been done to understand whether the brain distribution of lithium is in some way spatially localised. Whilst some studies have pointed towards localised effects of lithium; for example, it has been suggested that lithium might act in the hippocampus to promote neurogenesis (O'Leary et al., 2012), others have suggested that lithium exerts more widespread effects on white matter (Gildengers et al., 2015). Regional speci city of lithium action could in theory be underpinned by uneven distribution withevent issue sensitivity, even distribution but withuneven issue sensitivity, or an uneven distribution with uneven tissue sensitivity. A better understanding of brain lithium distribution may serve to support observations of regional speci city. The following section aims to introduce what is known about lithium distribution within the brain.

1.3.1 Histological studies

Preclinical studies

The study of lithium distribution within the brain has until relatively recently only been investigated in animals. Earlyex vivostudies using rats found that lithium was taken up by different organs in unequal amounts (Schou and Mogens, 1958) and that lithium is retained in bone following treatment cessation (Birch and Jenner, 1973). This led to a series of attempts to characterise lithium distribution within the brain using lithium-fed rats. Almost all of these studies reported lithium distribution to be “non-uniform” across the brain (Ebadi et al., 1974; Ebara and Smith, 1979; Edelfors, 1975; Hanak et al., 2015; Mukherjee et al., 1976; Nelson et al., 1976; Rios and Guzmanmendez, 1990; Smith and Amdisen, 1981; Thellier et al., 1980) with the exception of (Bond et al., 1975). While no consensus has been reached regarding which areas are thought to exhibit peak lithium concentrations certain patterns can be seen across these animal studies. For example, the hypothalamus and basal ganglia have been consistently found to contain greater lithium concentrations than the medulla and cerebellum (Ebadi et al., 1974; Edelfors, 1975; Mukherjee et al., 1976; Nelson et al., 1976; Rios and

Guzmanmendez, 1990), whilst another emergent trend appears to show increasing levels of lithium from hindbrain to forebrain (Ebara and Smith, 1979; Hanak et al., 2015).

Clinical studies

The first attempts to characterise lithium distribution in the human brain were performed using post-mortem tissue derived from patients with bipolar disorder (Francis and Traill, 1970; Spirtes, 1976). However, these studies reached different conclusions and interpretation was limited by low sample sizes (N = 2 and N = 1, respectively). Since the publication of these post-mortem studies, researchers did not begin to investigate lithium within the human brain until over a decade later (Renshaw and Wicklund, 1988). This gap was largely due to the inability to detect lithium *in vivo*. Currently, the only non-invasive means of doing so involves the use of magnetic resonance techniques.

1.3.2 ^{7}Lithium Magnetic Resonance Spectroscopy

Quantification of lithium in the brain *in vivo*, whilst challenging, can be performed using a technique called ^{7}Lithium Magnetic Resonance Spectroscopy (^{7}Li-MRS). MRS enables the non-invasive detection of various nuclei and compounds based upon their magnetic resonance properties by exploiting the fact that different nuclei possess different spins. This causes different chemical species to absorb radiofrequency energy at different frequencies depending upon their chemical structure and local environment. During MRS, broad wave radiofrequency energy is delivered to the target which is absorbed in different amounts depending upon the types and concentrations of compounds present. This energy is then emitted and detected by a receiver in the form of signal termed `free induction decay'. Following Fourier transformation of this signal a spectrum of different peaks is obtained whereby the position (termed chemical shift) and size of each peak corresponds to a particular chemical species and its relative concentration, respectively (Jackson, 1992).

The identification of different compounds and their relative concentrations based upon MRS spectra relies upon prior knowledge of expected chemical shifts and profiles of peaks. This technique is most commonly used to detect protons (^{1}H-MRS) as protons are present in most biologically active compounds. However, the same principles may be applied to detect ^{7}Lithium during ^{7}Li-MRS. Developments in the field of ^{7}Li-MRS have enabled the detection of lithium *in vivo* which, when compared to a reference sample of known concentration, can

be used to estimate lithium concentration within the brain. The *in vivo* detection of lithium using ^{7}Li-MRS was achieved by Renshaw and Wicklund (Renshaw and Wicklund, 1988). This study acted as proof of principle study showing that it was possible to quantify lithium in the human brain non-invasively.

Relationship between blood and brain lithium

Since the development of the ability to quantify lithium *in vivo*, the relationship between serum and brain lithium concentration has been investigated using ^{7}Li-MRS in both preclinical and clinical studies. Whilst preclinical studies have been fairly consistent in finding a positive correlation between serum and brain lithium (Komoroski, 2005), results from human studies have been more variable. For example, although there are a number of studies that have found positive correlations between serum and brain lithium concentration (Kato et al., 1994; Lee et al., 2012; Machado-Vieira et al., 2016; Moore et al., 2002), there are a few studies that report weak or no correlation (Riedl et al., 1997; Sachs et al., 1995; Soares et al., 2001). The study by Sachs *et al.*, however, found a positive relationship when all serum concentrations (including those which fell outside of the therapeutic range) were incorporated into the analysis. An attempt to examine this relationship over 48 hours (Plenge et al., 1994) found that brain lithium concentration varied in accordance with serum levels over this period, supporting the existence of a positive relationship between serum and brain lithium concentration in humans.

In addition to investigating the relationship between serum and brain lithium, other lines of research suggest that the ratio of concentration between lithium in plasma and red blood cells may be a more pertinent clinical marker when monitoring lithium therapy. Lithium passes red blood cell membranes through passive diffusion and via Na^{+}/Li^{+} counter-transport (Pandey et al., 1978) and there is some evidence to suggest that higher concentrations of lithium in red blood cells relative to plasma contributes towards therapeutic response and toxicity (Elizur et al., 1982; Frazer et al., 1978). However, such findings are limited and at present there is insufficient evidence to warrant the use of the red blood cell / plasma lithium ratio as a more effective clinical marker than the use of serum concentration alone (El Balkhi et al., 2009).

Whilst a failure to find a consistent relationship between serum and brain lithium concentration in human ^{7}Li-MRS studies may be explained by an individual variability in the

propensity for lithium to cross the blood-brain barrier, an alternative possibility may be that lithium does not exhibit a uniform concentration throughout the brain. Studies which have been performed using ^{7}Li-MRS are methodologically restricted to quantifying lithium concentration within certain prede ned areas of the brain due to the low spatial resolution and long acquisition times required. As a result, depending upon the study in question the region of the brain examined may differ. If lithium distribution throughout brain tissue is non-uniform, then studies which set their region of interest spanning different regions are expected to nd inconsistent results.

1.3.3 ^{7}Lithium Magnetic Resonance Imaging

Whilst ^{7}Li-MRS enables the detection of brain lithium *in vivo*, this technique faces a number of limitations such as its limited spatial resolution and long acquisition times. Although advances are leading to faster acquisition times, the time taken to post-process spectroscopic data means that ^{7}Li-MRS is still not routinely used in the clinic. The need for faster, higher resolution detection of brain lithium has led to advances in ^{7}Li-MRS such as ^{7}Li-MRSI (Lee et al., 2012), however, such techniques still require long acquisition times (46 minutes) and numerous post-processing steps.

^{7}Lithium exhibits a spectral singlet *in vivo*, a property which gives rise to the potential to apply conventional MRI approaches when imaging lithium. However, lithium's low tissue concentration and long T_1 time (Smith et al., 2011) means that standard acquisition protocols yield low signal to noise ratios. An acquisition protocol termed “balanced steady state free precession” (b-SSFP), however, is well positioned to detect species with such properties. In line with this, a novel acquisition technique (^{7}Li-MRI) has recently been developed which enables the detection of lithium *in vivo* in 8 minutes (Smith et al., 2018).

The development of ^{7}Li-MRI accompanied by its rapid acquisition speed and limited number of required post-processing steps makes this approach a signi cant step forwards in terms of its practical applications for clinical research. The rst application of this technique (Smith et al., 2018) has revealed that lithium exhibits a heterogeneous distribution across the brains of patients with bipolar disorder receiving long term lithium treatment (Figure 1.1).

Despite identifying heterogeneity in lithium distribution, this initial study using ^{7}Li-MRI was carried out in a small number of patients and hence further investigation into the distribution of

Fig. 1.1 ^{7}Li-MRI in eight subjects shown at the level of the head of the caudate nucleus (upper row), with corresponding ^{1}H-MRI axial slices (middle row). The combined images (lower row) show ^{7}Li-MRI (in cyan) overlaid on ^{1}H-MRI images. The distribution of lithium in the brain is heterogeneous in all subjects, and varies between subjects. Image taken from (Smith et al., 2018)

lithium is warranted. Averaged data across the subjects included in this study indicated higher lithium signal intensity in white matter compared with grey matter, and high signal intensity within the brain stem and corpus callosum, with notably low signal in the orbitofrontal cortex. However, a number of variables that were not controlled for during this study such as age, sex, comorbidities, concomitant medication and duration of treatment could all give rise to heterogeneity in lithium distribution. Moreover, whilst this technique demonstrated the ability to map whole-brain lithium, it only provided a snapshot of lithium distribution and did not explore the possible variability in distribution over time. In order to examine both the reliability of this technique and the stability of lithium distribution over time, Chapter 3 describes an original research study (Lithium Magnetic Resonance Imaging in Controls (LiMRIC)) whereby this point is addressed through the administration of therapeutic doses of lithium in healthy individuals.

1.4 Summary and aims of this thesis

The effects of lithium are many-fold and whilst it is clear that lithium is effective in treating bipolar disorder, it is not clear which of lithium's actions underpin this. In order to better characterise lithium's effects, a multi-modal approach can be advocated. With such an approach, the effects of lithium on the brain can be explored using a variety of metrics in parallel and synthesised to determine whether there is consistency in the observed effects on several putatively related parameters. Throughout this thesis original data acquired using a variety of MRI methodologies is presented. Chapter 2 aims to provide an introduction to structural MRI, quantitative MRI, diffusion MRI and ^{7}Li-MRI.

Current knowledge regarding the distribution of lithium in the brain is limited owing to the longstanding lack of technical ability to map brain lithium *in vivo*. The development of ^{7}Li-MRI enables research into brain lithium distribution to be undertaken with relative ease. However, owing to the novelty of this technique, its reliability has yet to be established. In line with this, Chapter 3 aims to establish the reliability of ^{7}Li-MRI and temporal stability of lithium brain distribution.

Whilst many proposals have been put forward with regards to the effects of lithium on the brains structural properties, one which has been repeatedly replicated is the ability of lithium treatment to promote white matter integrity, including a report which suggests that this action of lithium might be related to treatment response (Kafantaris et al., 2017). Chapter 4 aims to explore this further through quanti cation of the spatial relationship between local lithium concentration and white matter integrity using multimodal ^{7}Li-MRI and Diffusion MRI.

Quantitative relaxometry is another technique that can be used to study changes in tissue microstructure *in vivo* (see section 2.3). While there is some evidence to suggest that brain T_1 is elevated during BD and that lithium may reduce T_1, this effect has only been studied in relatively small cohorts. In order to further investigate this phenomenon, Chapter 5 reports on regional quanti cation of longitudinal T_1 in the brain of lithium treated and lithium-naïve patients with bipolar disorder in comparison to healthy controls.

Chapter 2

Magnetic Resonance Image analysis

2.1 Overview

Magnetic Resonance Imaging (MRI) is an umbrella term used to describe a range of images that can be acquired using an MRI scanner. In order to acquire such images, MRI takes advantage of a physical phenomenon known as nuclear magnetic resonance (NMR). Despite being underpinned by same NMR phenomenon, different acquisition protocols enable the quanti cation and study of a large range of properties in biological tissue. The ndings reported throughout this thesis were made possible by the extensive research and development of various MRI acquisition protocols.

Whilst a comprehensive description of this NMR phenomenon is beyond the scope of this work, the following chapter aims to introduce the various types of images that have been acquired as part of the research carried out during the production of this thesis. This introduction aims to provide an overview of these techniques, including a description of their potential applications during both clinical work and research, as well as their respective advantages and disadvantages.

2.2 T_1 and T_2 weighted images

The most routinely acquired MRI images are referred to as T_1 weighted (T_1w) and T_2 weighted (T_2w) images. T_1w and T_2w images of the human brain can be acquired rapidly

(typically in less than five minutes) and provide high resolution images of the brain which confer distinct tissue contrast (Figure 2.1).

T_1 and T_2 weighted images are termed as such owing to the resulting observable tissue contrast being predominately affected by either T_1 (longitudinal relaxation) or T_2 (transverse relaxation) processes. During proton imaging, T_1 relaxation is a time constant which describes the time taken for protons to relax back to equilibrium following excitation by an electromagnetic stimulus, while T_2 describes the time taken for excited protons to "dephase" with one another (McRobbie et al., 2006). T_1 and T_2 times differ according to the local magnetic field strength which is determined by factors such as scanner strength and composition of the local environment in which protons reside (Vymazal et al., 1992). MRI acquisition protocols designed to differ in terms of their sensitivity to T_1 and T_2 processes produce images in which resultant signals differ according to tissue type.

T_1 and T_2 weighted images can be differentiated visually according to the relative brightness of different tissue types. In most cases T_1 and T_2 weighted images may be distinguished by examining the brightness of the cerebrospinal fluid (CSF), with CSF appearing dark in T_1w images and bright in T_2w. However, this rule does not always apply, for example Fluid-Attenuated Inversion Recovery (FLAIR) sequences describes a type of acquisition protocol whereby the sequence is manipulated in order to nullify signal originating from the CSF, a feature that is useful for highlighting periventricular abnormalities.

.

2.2.1 Uses of T_1w and T_2w images

Clinical use

T_1 and T_2 weighted images are used routinely in the clinic owing to their speed of acquisition, high resolution and excellent tissue contrast that they confer. They can be used to identify structural abnormalities such as tumours or lesions. For example, FLAIR images can be used to highlight white matter hyper-intensities, a structural abnormality found to be more prevalent in patients with bipolar disorder (Ahn et al., 2004).

Fig. 2.1 Top: Axial slices depicting a T_1 weighted image (above) and a T_2 weighted image (below).

Use in research

T_1w images are almost always invariably acquired alongside the acquisition of any other additional image types during brain imaging studies owing largely to their ability to facilitate image co-registration and tissue segmentation. A large number of linear and non-linear image registration algorithms (Klein et al., 2009) have been speci cally developed to enable the registration of T_1w images of the brain to one another. The need for image registration arises during both cross-sectional group studies and longitudinal studies. For example, in order to track changes in the same region of the brain of a given individual over time during multi-session studies, multiple images from the same individual must be co-registered to one another. Intra-subject co-registration can be performed using linear registration algorithms which permit rotation, translation, zooming and shearing of the data. In contrast, during cross-sectional studies brain images from multiple subjects are typically aligned into a common space. During the co-registration of multiple subjects, non-linear warping algorithms are required. Non-linear registration permits local deformation of the data enabling images from multiple individuals to be warped to match a common template. Such non-linear registration involves greater distortion of the original data than linear registration and is therefore a limitation of group analyses which are performed in standard space.

The excellent contrast between grey and white matter that T_1-weighted images offer means that these images are routinely used for tissue segmentation. Segmentation of brain images enables the morphometry of individual anatomical structures to be quanti ed. For example, segmentation of subcortical nuclei can be used to compare the volume of such structures between individuals and over time. This can now be achieved with relative ease owing to the development of software packages such as Freesurfer (https://surfer.nmr.mgh.harvard.edu/). As a result, brain morphometry parameters such as cortical thickness, curvature, volume and surface area are increasingly becoming commonly reported metrics in brain imaging studies.

Freesurfer comprises a set of tools which enable the mapping of the cortical surface and subcortical structures. The Freesurfer processing pipeline consists of two main streams, the “surface-based” stream and “volume-based” stream. The function of the surface-based stream is to map the boundaries between white matter, cortical grey matter, and the pial surface (Figure 2.2A) and parcellate cortical structures, whilst the function of the volume-based stream is to segment and label subcortical tissue structures (Figure 2.2B). Both streams achieve this through a series of steps comprising linear registration with the with the MNI305 atlas (Collins and Evans, 1994), image intensity normalisation via assessment of signal variation across white matter volume (Sled et al., 1998), and intensity-based voxel classi cation (Dale et al., 1999).

During cortical segmentation and parcellation, brain areas can be subdivided and labelled in a variety of ways based upon common atlases. Voxel classi cation is driven by assigning a probability based upon pre-determined labels that are encoded within a training set. By default there are three atlases which are included within the Freesurfer processing pipeline: the Desikan-Killiany cortical atlas (Desikan et al., 2006), Destrieux atlas (Destrieux et al., 2010), and Desikan–Killiany–Tourville atlas (Klein and Tourville, 2012). Brain atlases vary in terms of the number of regions that they contain which may be determined by anatomical landmarks such as gyri and sulci, local cytoarchitecture, patterns of connectivity or functionally specialised regions.

Fig. 2.2 (A) Freesurfer cortical reconstruction of the pial surface and white matter boundary. Cortical thickness is estimated by calculating the distance between the outer pial (red) and white matter surface (yellow) . (B) Freesurfer parcellation based upon the Destrieux atlas.

2.2.2 Limitations

The major limitation associated with T_1 and T_2 weighted imaging arises from the fact that, unlike quantitative imaging (see section 2.3), signals obtained are not absolute and T_1 and T_2 weighted images are optimised to produce maximal grey/white matter tissue contrast, meaning that comparison of signal intensity between sites, protocols, scanners, and time points is challenging. There are also limitations when it comes to comparing metrics such as cortical thickness and volume between sites and over time. For example, signal degradation and changes in image intensity have been shown to occur over time in a phenomenon known as scanner drift (Hansen et al., 2019). Scanner drift has been shown to in uence volumetric measurements (Takao et al., 2011) and scanner model has also been shown to affect measure of cortical thickness, meaning that this is something which should be controlled and corrected for during multi-site studies (Fortin et al., 2018). When using Freesurfer to de ne regions of interest, errors may be introduced as poor image contrast can cause Freesurfer to incorrectly classify tissue types during segmentation and parcellation. To limit this, regions of interest can be eroded to minimise the inclusion of misclassi ed voxels and images should also be inspected visually post-segmentation by trained individuals.

.

2.3 Quantitative relaxometry

Quantitative relaxometry refers to the quanti cation of relaxation times, such as T_1 and T_2. Unlike, T_1 and T_2 weighted images, which modulate acquisition sequences in order to

optimise image contrast, signals acquired during quantitative MRI sequences (qMRI) directly correspond to an absolute quantitative measure of time (Deoni, 2010).

The gold standard method used to quantify T_1 and T_2 relaxation involves the use of an acquisition sequence known as “Inversion Recovery”. Inversion recovery sequences characterise relaxation times by inverting the magnetic moment of protons using a radiofrequency (RF) pulse and measuring the time taken for net magnetisation to fully recover. To achieve this, a 180° RF pulse is used to fully invert the net magnetisation vector (Figure 2.3A). Over time this net magnetisation starts to recover at a rate determined by T_1, during which time the net magnetisation will pass through a null point (Figure 2.3B) . In order to characterise the T_1 recovery curve, a single 90° RF pulse is applied during each recovery at varying intervals. Through repetition of this process, the extent of recovery may be determined by recording and plotting the net magnetisation following this RF pulse. For example, if a 90° pulse is applied at the null point, net magnetisation becomes fully inverted once again, whereas if a 90° pulse is applied following full recovery (Figure 2.3C), net magnetisation will return to zero.

Fig. 2.3 Following a 180° RF pulse net magnetisation is inverted (A), during recovery this passes through a null point (B) before finally recovering to equilibrium magnetisation (C). The time taken to fully recover is the T_1 time.

Whilst inversion recovery sequences are able to accurately quantify relaxation time, this process takes a long time as it requires waiting for the full recovery of magnetisation. In order to overcome this, a range of newer acquisition protocols have been developed which enable an estimation of relaxation rates whilst minimising acquisition time.

Driven Equilibrium Single Pulse Observation of T_1 (DESPOT1) is an example of such a sequence (Deoni et al., 2005). DESPOT1 works on the basis that signal intensity in Spoiled Gradient Recalled-Echo (SPGR) images (SI_{SPGR}) can be modelled on equations relating the density of protons within a given voxel (proton density), longitudinal relaxation (T_1), the length of time between the application of excitation pulses (repetition time, TR), the rotation of the net magnetisation vector (flip angle, α), and, M_0, a factor proportional to the equilibrium longitudinal magnetisation (Equation 2.1).

$$\frac{SI_{SPGR}}{\sin\alpha} = \frac{SI_{SPGR}}{\tan\alpha} E_1 + M_0(1 - E_1) \; ; \quad \text{where} \quad E_1 = e^{-\frac{TR}{T_1}} \tag{2.1}$$

Using the DESPOT1 approach, T_1 parameter maps are produced via the acquisition of two consecutive images during which the TR is held constant but the flip angle is modified. This means that two values (x_1, y_1 and x_2, y_2, Equation 2.2) are obtained for which the slope between these points is equivalent to E_1 (Equation 2.3).

$$\begin{aligned} y_1 &= \frac{SI_{SPGR_1}}{\sin\alpha_1} \quad y_2 = \frac{SI_{SPGR_2}}{\sin\alpha_2} \\ x_1 &= \frac{SI_{SPGR_1}}{\tan\alpha_1} \quad x_2 = \frac{SI_{SPGR_2}}{\tan\alpha_2} \end{aligned} \tag{2.2}$$

$$\text{slope} = E_1 = \frac{(y_2 - y_1)}{(x_2 - x_1)} \tag{2.3}$$

As a result, by rearranging E_1 to the form shown in Equation 2.4, T_1 may be calculated by measuring the slope of this line.

$$T_1 = \frac{TR}{\ln(\text{slope})} \tag{2.4}$$

2.3.1 Uses of qMRI

The development of rapid acquisition quantitative sequences means that qMRI is now becoming feasible in a clinical context. One of the major advantages of qMRI over qualitative imaging includes the ability to directly compare image signal intensity over multiple time points and between acquisition sites. T_1 and T_2 relaxation serve as quantitative measures which are sensitive to myelin, macromolecular content, iron and water content. As a result, changes in relaxation may act as biomarkers which represent an underlying pathology. For example, studies have used quantitative relaxometry to identify changes in iron content during Parkinson's disease (Lee et al., 2018), visualise excess water content in malignant gliomas (Blystad et al., 2017), map demyelination during multiple sclerosis (Manfredonia et al., 2007), and detect hippocampal sclerosis during temporal lobe epilepsy (Jackson et al., 1993).

2.3.2 Limitations

Whilst rapid acquisition qMRI protocols have been developed, results from studies which use different acquisition sequences do not always match the gold standard inversion recovery method (Tsialios et al., 2017). As such, studies which cross-compare and pool results between sites must ensure that the same acquisition protocols and local environments are maintained.

Another important factor to consider when applying qMRI is partial volume effects. Different tissues vary greatly in terms of relaxation rate, and therefore if regions of interest contain multiple tissue types results may become skewed. When using a segmentation based approach based upon a T_1w image, the means of de ning a region of interest (ROI) can become circular. This is because regions of interest are determined based upon a contrast weighted image which, in turn, is determined by factors affecting T_1 and T_2. In Chapter 5 we address this challenge by using an ROI erosion approach whereby the outer surface voxels for each individual ROI were excluded from the analysis.

2.4 Diffusion MRI

Diffusion weighted magnetic resonance imaging (dMRI) describes a type of acquisition sequence designed to be sensitive to the diffusion of water molecules. The diffusion (also termed “brownian motion”) of water describes the random displacement of water molecules as they become agitated by thermal energy (Einstein, 1905). Owing to the fact that the diffusion of water within the cellular space is restricted relative to extracellular water, measuring how the diffusion of water differs across biological tissue enables inferences to be made with regards to the brain's axonal structure.

The main principal underpinning dMRI involves the collection of multiple images whilst exposing the target to magnetic eld gradients in differing spatial directions. When a magnetic eld is applied to tissue, vectors of the spin polarisation begin to precess at a rate proportional to the strength of the local magnetic eld. As a result, when a magnetic eld is applied in the form of a spatial gradient, this causes neighbouring protons to precess at different rates and subsequently become out of phase with one another. Diffusion MRI exploits this phenomenon by applying two consecutive magnetic gradients of equal strength in the opposite spatial direction to one another. This results in an effect such that if no diffusion had occurred during this time then all protons should “re-phase” with one another. As a result, by measuring the relative extent of “re-phasing” (which is measured in terms of signal strength) a spatial map corresponding to the local levels of molecular diffusion can be generated. The type of map is known as the Apparent Diffusion Coef cient (Patric Hagmann, 2006).

In addition to being able to quantify the extent of diffusion in the brain, dMRI also enables an estimation of the relative direction or “anisotropy” of diffusion. An estimate of anisotropy is made possible by the acquisition of images exposed to magnetic gradients in multiple orthogonal directions. The characterisation of the diffusion pro le of water can be achieved by modelling a second order tensor (T) based on diffusion along the Cartesian axes x, y and z (Equation 2.5). In the case of fully isotropic diffusion, this tensor becomes proportional to a 3 x 3 identity matrix.

$$T = \begin{pmatrix} T_{xx} & T_{xy} & T_{xz} \\ T_{yx} & T_{yy} & T_{yz} \\ T_{zx} & T_{zy} & T_{zz} \end{pmatrix} \quad (2.5)$$

The eigenvalues and eigenvectors associated with this tensor represent the magnitude and direction of diffusion at a given voxel. The calculation of such eigenvalues have provided useful metrics when it comes to the quanti cation of anisotropy. For example, a commonly reported parameter during dMRI studies is Fractional Anisotropy (FA), a measure which describes the fraction of the diffusion tensor magnitude driven by anisotropic diffusion. Fractional anisotropy is a normalised parameter which ranges between 0-1, and in order to estimate FA dMRI acquisition protocols must ensure to have at least six non-collinear magnetic spatial gradients. The calculation of FA is given in Equation 2.6, whereby λ represents the three eigenvalues associated with the x, y and z axes and $\bar{\lambda}$ represents the mean eigenvalue.

$$FA = \sqrt{\frac{3}{2}} \sqrt{\frac{(\lambda_1 - \bar{\lambda})^2 + (\lambda_2 - \bar{\lambda})^2 + (\lambda_3 - \bar{\lambda})^2}{\lambda_1^2 + \lambda_2^2 + \lambda_3^2}} \quad (2.6)$$

High levels of FA are found in white matter tracts whereby axons align in the same direction. However, although FA has been shown to be associated with white matter integrity (Song et al., 2008), it is a limited measure when it comes to studying areas which contain crossing bres. In order to address this issue, advances in the modelling of diffusion have led to the development of a parameter known as “generalised FA” (gFA) (Tuch, 2004). Generalised FA has been shown to better characterise white matter integrity in areas containing crossing bres by modelling diffusion using a higher order orientation distribution function. Changes in FA and gFA within white matter have been found to occur in a large number of disorders, including bipolar disorder (see Chapter 4).

2.4.1 Uses of dMRI

Clinical use

Although widely used throughout research, dMRI is less commonly used in the clinic. Amongst the reasons for this current lack of translation include its relative novelty as a

technique and the need for signi cant image post processing in comparison to T_1 and T_2 weighted images. For example, parameter maps need to be generated and co-registered to structural brain images before meaningful anatomical data can be extracted (Figure 2.4 A and B). One of the clinical uses of dMRI which is in the process of being applied is during neurosurgery (Conti Nibali et al., 2019). Owing to the ability to model structural connectivity with high levels of detail, neurosurgeons are able to use this map as a tool when performing surgery in order to minimise damage to major axonal tracts (Costabile et al., 2019). Diffusion MRI is also useful clinically during the detection of damaged regions following a stroke (Alegiani et al., 2019). During stroke, shutdown of the Na^+/K^+ pump, leads to a net in ux of water into the cell causing water to become more restricted in terms of its ability to diffuse randomly. As a result, ischaemic regions of brain tissue present as dark spots on ADC parameter maps.

Use in research

The ability to model the direction and strength of the diffusion of water molecules enables the characterisation of white matter microstructural properties and structural connectivity in vivo. In addition to fractional anisotropy, there are a variety of other parameters that may be extracted when tting a diffusion weighted tensor, including radial diffusivity (RD), axial diffusivity (AD) and mean diffusivity (MD). Such parameters have been found to re ect different microstructural properties. For example, axonal injury is associated with a reduction in FA and AD (Song et al., 2008), demyelination has been associated with increased RD (Budde et al., 2007; Song et al., 2005), and increased myelination has been shown to correspond with an increase in FA (Chang et al., 2017).

Owing to the fact that dMRI derived parameters can provide markers of microstructural integrity, research has been undertaken to characterise how such properties differ in the brain during health and disease. There are a number of approaches that may be used when attempting to quantifying such differences. For example, using a ROI approach, parameters may be compared across a series of atlas based segmentations (Figure 2.4C). In Chapter 4 this approach is taken in order to quantify the differences in generalised FA between patients with bipolar disorder and healthy controls across regions de ned by the John Hopkins University (JHU) white matter atlas. This ROI approach is useful as it enables ndings to be readily cross-compared between studies. Additionally, the JHU atlas contains core regions of white

matter which are not located in regions highly susceptible to image distortion such as the orbitofrontal cortex (see section 2.4.2).

An alternative to the ROI based approach includes a voxelwise analysis, whereby parameters such as FA are compared on an individual voxel basis. However, in order to do so images from multiple subjects need to be accurately co-registered to one another. Moreover, owing to the large number of comparisons being made during such analyses, statistical methods are needed to account for the false positives. A popular approach to the voxelwise analysis of dMRI data has been developed, known as “Tract Based Spatial Statistics” (Smith et al., 2006). Tract Based Spatial Statistics addresses these issues by projecting individual subject FA maps onto a “mean FA skeleton” which represents the central point of all tracts common to the group. This skeleton is then subject to voxelwise cross subject statistics. This approach minimises the number of comparisons being made whilst also aiming to maximise the accuracy of between-subject registration.

The ability to detect the direction of diffusion using dMRI to infer axonal tracts has led to the development of a method of analysis known as tractography. Tractography describes the mapping of discrete bre tracts throughout the brain, enabling a characterisation of brain-wide structural connectivity. The potential applications of this technique are far-reaching, for example, graph theoretical methods are increasingly being used to quantify differences in the structural connectome between patient and controls (O'Donoghue et al., 2017). However, owing to rapid development of this eld there currently exists a large number of bre-tracking algorithms each liable to generate different results (Jeurissen et al., 2019). As such, the relationship between the dMRI-derived structural connectome and true anatomy warrants further investigation.

Fig. 2.4 (A) Raw diffusion MRI volumes are first corrected for image distortion and processed to obtain meaningful parameters such as gFA. (B) Parameter maps are then co-registered to either the individual subject ^{1}H image or standard space. (C) Co-registered parameter maps may then be used to perform regional analysis of diffusion parameters.

2.4.2 Limitations

In addition to the need for significant post-processing, diffusion weighted acquisition sequences are also susceptible to image distortion as dMRI falls under a type of imaging sequence known as "Echo planar Imaging". Echo planar imaging sequences enable the acquisition of a single image in under 20 milliseconds (DeLaPaz, 1994); however, this comes with the disadvantage of being extremely sensitive to movement and susceptibility artefacts. For example, orbito-frontal regions appear distorted on dMRI images due to inhomogeneities in the magnetic field caused by the neighbouring air-filled cavity. Whilst this can be overcome to some extent via the collection of fieldmaps (Rohde et al., 2004), results gained from dMRI nearing such regions should be interpreted with caution.

2.5 ^{7}Li-MRI

The recent development of ^{7}Li-MRI (Smith et al., 2018) marks a step forward in terms of speed of acquisition and image resolution when it comes to detecting lithium *in vivo* compared with ^{7}Li-MRS (see section 1.3.2). However, despite this there are a number of factors to consider when applying this technique.

As with ^{1}H-MRI, ^{7}Li-MRI signal intensity is determined by T_1 and T_2 relaxation processes in addition to lithium concentration and therefore does not represent a measure which can be easily translated back into mmol/L. Despite this, results from phantom studies show a direct correlation between ^{7}Li-MRI signal intensity and lithium concentration in pure samples (Smith et al., 2018) and as such, voxels containing uniform tissue properties should exhibit ^{7}Li-MRI signal that directly corresponds with lithium concentration.

The resolution of ^{7}Li-MRI, albeit higher than ^{7}Li-MRS, remains lower than well established image acquisition protocols such as diffusion MRI. For example, typical dMRI protocols acquire images at 2mm^3 isotropic resolution, whereas the reconstructed voxel size for ^{7}Li-MRI is 20mm x 20mm x 25mm. As a result, a large proportion of ^{7}Li-MRI voxels will contain mixed tissue types making results susceptible to partial volume effects (Figure 2.5). When processing ^{7}Li-MRI images at the current resolution care must be taken to ensure that partial volume effects are accounted for. In Chapter 4 this is achieved using a tissue segmentation approach whereby lithium voxels are treated separately depending upon their individual tissue composition.

Fig. 2.5 Figure showing raw (non-interpolated) ^{7}Li-MRI image, illustrating an example of partial volume effects. Each ^{7}Li-MRI voxel (top row) contains a mixture of tissue types when overlaid onto the co-registered T_1W image.

2.6 Discussion

The methods used throughout this thesis and described within this chapter comprise only a small proportion of available MRI techniques and new acquisition protocols continue to be developed and optimised. Whilst the development of new techniques is undoubtedly a good thing in that it enhances the toolkit which may be used to study the brain, an expanding number of tools also comes with challenges in terms of how best to use them.

The ability to derive multiple parameters using the same acquisition protocol means that despite acquiring the same image type, independent studies may choose to report different parameters. For example, within the diffusion MRI literature, some studies choose to report fractional anisotropy, whilst others choose to report changes in generalised fractional anisotropy or mean diffusivity. As such, researchers are faced with a challenge of cross-comparability between studies when different studies choose to report different post-processing parameters. Additionally, the wide variety of readily available post-processing methods poses a disincentive to replicate findings when researchers can instead declare a "novel" finding by simply reporting a new parameter. Factors such as this may be amongst the reasons contributing to the current crisis in replicability (Baker, 2016). Given commonalities in processing pipelines, novel analysis techniques could readily be presented alongside more robustly established methods to strengthen comparison and better understand the evolution of the findings.

The ongoing rapid development of new techniques also means that studies can often disseminate new findings before thoroughly validating a technique. The reliability and consistency of techniques should be repeatedly and independently validated before inferences can be made. To this end, we report on the within subject scan-rescan reliability of T_1-MRI in Chapter 3.

Finally, whilst a greater number of parameters can reveal more about biological properties in vivo, in order to be able to interpret such properties there is a need for further studies to directly relate changes in observable imaging parameters to biological changes. The biological changes underpinning dMRI derived parameters have been relatively well characterised during preclinical studies, with results linking increased fractional anisotropy to white matter integrity and myelination; however, changes in T_1 which are detected using quantitative MRI remain challenging to interpret.

Chapter 3

Lithium Magnetic Resonance Imaging in Controls (LiMRIC)

3.1 Abstract

The development of a novel non-invasive imaging technique (^{7}Li-MRI) has enabled rapid imaging of lithium distribution within the human brain (Smith et al., 2018). A preliminary study using this technique has shown that lithium exhibits a non-uniform distribution across the brain of patients with bipolar disorder undergoing long term lithium treatment. However, the scan-rescan reliability of ^{7}Li-MRI has yet to be investigated; it is also not known whether this pattern of distribution remains stable over time, nor whether brain lithium is detectable using ^{7}Li-MRI following short term administration of lithium.

The aims of the LiMRIC study were to establish the scan-rescan reliability of ^{7}Li-MRI and determine the stability of lithium distribution over time. To do so, healthy male subjects were administered with lithium for two weeks and scanned using ^{7}Li-MRI on three occasions during the final week.

The results showed that lithium exhibited a non-uniform distribution in all subjects. ^{7}Li-MRI images exhibited high variability in terms of raw signal magnitude between scans, but the pattern of lithium distribution was comparable. A greater degree of correlation was seen during within-subject comparisons when compared with between-subject comparisons;

however, moderate correlations were also observed between subjects following smoothing ($r^2 > 0.6$).

This study demonstrated that lithium distribution is detectable using ^{7}Li-MRI following short term lithium administration and the pattern of lithium distribution appears to remain stable over the course of one week, supporting the use of this technique during short term studies. However, variability in raw signal magnitude suggests that future analyses should be performed on an individual subject basis, or signal normalisation should be performed prior to any comparison of signal magnitude. Studies that aim to co-register multiple images should consider applying smoothing to account for voxel mismatch and take care to account for partial volume effects.

3.2 Background

The recent development of a novel magnetic resonance lithium imaging technique, ^{7}Li-MRI (Smith et al., 2018), enables researchers to image lithium *in vivo*. The aforementioned study using this technique showed that the distribution of lithium within the brain of patients with bipolar disorder taking lithium is heterogeneous and high lithium signal intensity was found in white matter, notably in the brain stem and corpus callosum; however, the source of the observed heterogeneity is currently unknown. Whilst it is possible that such heterogeneity is re ective of a true biological difference in individual uptake and handling of lithium, it is also possible that such variability is caused by poor reproducibility of this technique.

^{7}Li-MRI has thus far only been applied to patients with a diagnosis of bipolar disorder receiving long-term lithium treatment. This introduces a number of potential confounders including duration of lithium use and disease severity. Moreover, this technique has not yet been used to determine how lithium distribution varies over time. The following study aims to address these outstanding unknowns by using this novel technique to image lithium within the brains of healthy individuals with no prior history of lithium use. Healthy male volunteers were administered lithium for two weeks and scanned repeatedly over the course of the nal week. The aims of this approach were to determine whether lithium is detectable following short term lithium administration and to establish the scan-rescan reliability of ^{7}Li-MRI. This was addressed across multiple time scales including within the same day, over 24 hours, and over the course of a week.

3.3 Methods

3.3.1 Participants

Four healthy male volunteers (HC) were recruited to the LiMRIC study (ages 21, 24, 25 and 45). The subjects had no history of psychiatric illness and were not taking any psychotropic medications. Subjects were screened using the Mini-International Neuropsychiatric Interview (v7.0) by a trained clinical research assistant (Amy-Rose Hayes). Exclusion criteria were contraindications to magnetic resonance examination, current or recent harmful drug or alcohol use, comorbid psychiatric diagnosis, learning disability or impairment of capacity. All subjects provided written informed consent and the study was granted a favourable ethical opinion by a United Kingdom National Research Ethics Committee (18/SW/0033) and sponsored by Northumberland, Tyne and Wear NHS Foundation Trust. This study was audited in March 2019.

Lithium administration

All subjects were prescribed lithium carbonate (Priadel™ modified release once daily), initiated without titration based upon a dose calculated using the Cockcroft-Gault method (Chiu et al., 2007) but capped at a maximum dose of 1000mg per day to ensure safety. The Cockcroft-Gault method requires an estimate of kidney function, measured using a blood sample taken during participant screening. Serum lithium levels were checked on three occasions (study days 7, 8 and 14) by standard bloodletting. Subjects were instructed to take their lithium dose at 9pm each evening and serum lithium sampling was performed at 9am immediately prior to scanning. The therapeutic range in clinical practice is based upon samples taken 12 hours post-dose. Our procedure replicated this, enabling direct comparability between serum levels and therapeutic reference ranges. This also provided standardisation of sampling with respect to lithium clearance across subjects ensuring that any effects relating to brain lithium uptake were comparable between subjects. Participants attended three 9.30am scanning sessions (study days 7, 8 and 14). During each session, two ^{7}Li-MRI and ^{1}H-MRI T_1w structural scans were acquired. An outline of the experimental timeline is given in Figure 3.1.

Fig. 3.1 LiMRIC experimental design. Following an initial assessment, lithium was taken for a period of seven days before the first scan session. Blood samples to determine serum lithium concentration were taken on days 7, 8 and 14. ^{7}Li-MRI took place on days 7, 8 and 14. Each scanning session included two back-to-back ^{7}Li-MRI and ^{1}H-MRI T_1w structural scans. The final dose of lithium was taken on the evening of day 13.

3.3.2 Image acquisition

Scanner and coil systems

All MR data were acquired on a Philips 3T Achieva scanner (Philips Medical Systems, Best, The Netherlands) with ^{1}H structural and ^{7}Li-MRI imaging performed using a double tuned ^{1}H / ^{7}Li radiofrequency (RF) birdcage head coil (RAPID Biomedical, Rimpar, Germany).

T_1w image acquisition

High resolution T_1w: 3D T1-weighted images of brain anatomy were acquired immediately prior to ^{7}Li-MRI imaging. The first T1-weighted image was acquired with a ^{1}H gradient echo sequence using the following parameters (TR = 9.6 ms, TE = 4.6 ms, FOV = 240 x 240 x 180 mm^3, acquisition matrix = 240 x 208 x 180, acquisition voxel size = 1 x 1.15 x 1 mm3, reconstructed into a matrix size of 256 × 256 × 180, 1 average).

Low resolution T_1w: The second T_1w image was acquired at half the resolution of the high resolution T_1w image in the z plane. All other acquisition parameters were kept the same. This enabled rapid acquisition and provided sufficient spatial resolution for accurate within-subject linear registration.

^{7}Li-MRI acquisition

Prior to data acquisition, correct radiofrequency power calibration was con rmed on a per-subject basis with a ^{7}Li ip angle calibration. Non-localised ^{7}Li spectra were acquired at six ip angles between 30 and 180 degrees. A sinusoidal function was tted to spectral peak amplitudes to determine discrepancy between requested and achieved ip angle. Based upon the results of this calculation, requested ip angles were 51° for all subjects except MR03 for whom the requested ip angle was 54°. ^{7}Li-MRI data acquisition commenced immediately after T_1w structural image sequences. ^{7}Li-MRI was acquired using a protocol constructed for maximal ^{7}Li signal amplitude (FOV = 480 × 480 × 175 mm^3, 20 × 19 × 7 acquisition matrix and 24.0 x 25.3 x 25.0 mm^3 voxel size, with TR = 9.4 ms, TE = 4.5 ms, receiver bandwidth = 219 Hz/pixel, 500 averages per dynamic, 3 dynamics). Data were reconstructed into a 32 × 32 × 7 matrix with a voxel size of 15 × 15 × 25 mm^3. The sequence, lasting approximately eight minutes, was conducted thrice without a notable interval and the three scan dynamics were averaged in complex form.

Scanning protocol

Scan sessions took place on study days 7, 8 and 14. On study days 7 and 8, ^{7}Li-MRI scans were taken in order to investigate the effect of removal from scanner on scan-rescan reliability. On study day 7 subjects remained in the scanner throughout the whole session. On study day 8 subjects were removed and repositioned in the scanner following acquisition of the rst ^{7}Li-MRI scan. On study day 14 two scanning blocks were completed, but the nal block was used for sequence development for a different project not presented here. An outline of the scanning protocol is shown in Figure 3.2.

Fig. 3.2 LiMRIC scan protocol. During each session a T_1w image acquisition preceded ^{7}Li-MRI acquisition. The first T_1w acquisition was high resolution. On study day 7 subjects remained in the scanner throughout the whole session. On study day 8 subjects were removed and repositioned into the scanner between ^{7}Li-MRI scans.

3.3.3 Image processing and analysis

T_1w and ^{7}Li-MRI images were exported in DICOM format and converted to NIFTI format data using MRIconvert version 2.0 for Windows (Lewis Center for Neuroimaging, University of Oregon, OR, USA). ^{7}Li-MRI data for MR02 Day 7 Scan 2 was unavailable due to file corruption during export from the scanner. Data pre-processing and analysis were performed using Nipype, a Python based platform that provides a uniform interface to existing neuroimaging software and facilitates interaction between these packages within a single workflow (Gorgolewski et al., 2011).

Image resampling and co-registration

The T_1w images of each subject were linearly co-registered to their respective initial T_1w image collected during the first imaging session (study day 7) using FMRIB's Linear Image Registration Tool (Jenkinson et al., 2012). ^{7}Li-MRI images were resampled to the resolution of the T_1w image using nearest neighbour and linear interpolation. Linearly interpolated images were used for display purposes, whilst all analyses were performed using nearest neighbour interpolated images. Resampled ^{7}Li-MRI images were then transformed by applying the transformation matrix obtained from registering the structural T_1w images to the T_1w image collected during study day 7.

Image post-processing

Co-registered ^{7}Li-MRI images were masked for brain-only voxels using a binary mask generated by applying FSL's Brain Extraction Tool to the co-registered ^{1}H T$_1$w image (Smith et al., 2002). Following masking, ^{7}Li-MRI images were smoothed using a Gaussian kernel of full width half maximum sizes ranging from 0mm - 4mm in increments of 1mm. ^{7}Li-MRI images were then downsampled to the original ^{7}Li-MRI resolution.

An estimation of noise per ^{7}Li-MRI image was achieved by averaging all background signal. To do so, the FSL "outskin mask" function was used to obtain a mask encompassing all bodily tissue. The inverse of this mask was subsequently used to sample background signal.

Quantification of cross-scan comparability

Brain voxels from co-registered downsampled ^{7}Li-MRI images were regressed against one another in order to determine the correlation between separately acquired ^{7}Li-MRI images. Between scan correlation was assessed within the same session (removed from scanner vs remained in scanner) and between sessions (study days 7 vs 8 vs 14). In order to establish a reference point, the same process was applied to corresponding ^{1}H T$_1$w images.

MNI space analysis

In order to conduct a between-subject comparison, ^{7}Li-MRI images were additionally registered to the Montreal Neurological Institute standard space brain template (2mm resolution). This was achieved by non-linear warping of every ^{1}H T$_1$w image from every subject and session individually to this template using FMRIB's Non Linear Image Registration Tools (Jenkinson et al., 2012). The resulting transformation matrix was then used to transform every resampled ^{7}Li-MRI image individually. Standard space co-registered images were smoothed and downsampled to the original ^{7}Li-MRI resolution following the same post-processing steps as during the within-subject analysis.

The correlation between ^{7}Li-MRI brain voxels was calculated pairwise for all combinations of images which were classified as either "within" or "between" subject. A schematic illustrating the resulting variations of comparisons is given in Figure 3.3. Significance between the difference in r^2 values for within versus between subject comparisons was tested using a Wilcoxon signed rank test after confirmation that data was non-normally distributed using the Lillefors test of normality.

Fig. 3.3 Schematic illustrating how difference combinations of within vs. between subject ^{7}Li-MRI comparisons were generated. Pearson r^2 values were computed for all various combinations of ^{7}Li-MRI image comparisons and classified as either “within” or “between” subject.

3.4 Results

3.4.1 ^{7}Li-MRI raw scans

^{7}Li-MRI raw images for subjects MR02, MR03, MR04 and MR05 are shown in Figures 3.4, 3.5, 3.6 and 3.7, respectively. Some degree of consistency in terms of the pattern of the lithium distribution can be seen visually both within and between subjects.